



MACHINE LEARNING BASED TECHNIQUE TO LEARN HIPPOCAMPAL ATROPHY FROM AXIAL MRI FOR ALZHEIMER'S DISEASE DIAGNOSIS

D. K. RAMKUMAR *, N. V. BALAJI † AND T. GENISH ‡

Abstract. Hippocampus (HC) is one of the small brain components and its features majorly take part in diagnosing diseases such as Alzheimer and Dementia. The earlier detection of the size changes of HC leads to take preventive action against Alzheimer disease at initial stage. Thus the HC voxel quantification becomes essential to know the severity of the disease and thus induces computerized segmentation process. Several semi-automatic and automatic HC segmentation techniques proposed earlier. Though, it requires large memory space and high computational cost. This paper reduces the risk of searching a high configuration machine and reduces the cost by utilizing limited number of features. It is to be done by using some strategic features based on mathematical framework of wavelet, statistical features and gray level computations called level set. The features fed as input to the supervised machine learning model called back propagation neural network. A deep study conducted to train the net and analyzed in various views. The results were compared with the similar existing models which were using Random forest, Quicknat and deep learning. The proposed machine learning model produces the higher and similar dice scores of existing model. The validation of the proposed method yields 85% of dice score and 96% of sensitivity and 96% of specificity.

Key words: segmentation, features, back propagation algorithm, hippocampus .

AMS subject classifications. 68T05

1. Introduction and examples. Hippocampus (HC) is one of the brain regions and incorporates in memory function and it owns the structure of sea horse [19]. The hippocampus supports to know the age of a person [5]. Hence, the size of HC is notable one because some neurological diseases such as dementia and Alzheimer cause the size loss [7]. Further, the size of HC indicates the diseases like epilepsy and schizophrenia [2]. Alzheimer is one of the brain disorders, which affects memory power and cognitive skills. It easily affects hippocampus (HC) than other brain parts. In the entire world, 90 million peoples have suffered by Alzheimer disease [14]. The volume detection process of HC ensures the progressiveness of Alzheimer and guide to prevent its progression. At present, Magnetic Resonance Imaging (MRI) is non-invasive technology to mimic (capture) the morphology of human organs particularly brain [14]. The manual quantification of HC tissues from MRI images are consuming more times and tired the Radiologists. Hence, the necessity of computer aided methods for automatic segmentation is increasing exponentially. Though, the process of segmenting Hippocampus is very difficult [22].

The difficulties faced by automatic segmentation are noise, resolution constraint and weak boundaries between the brain components. When they are in same intensity, the pixels are not unique in intensity and not defined by a well defined boundary. The hippocampus segmentation methods are broadly categorized into i) Atlas and mullti-Atlas based method, ii) Deformable models such as Active contour models (ACM), Active shape model (ASM) and active appearance model (AAM) which uses local neighbourhood features and iii) Machine learning (ML).

ML is a rising technology which requires a set of features from a dataset to train the network and obtain optimal parameters in training stage, utilizes these parameters to detect objects from unknown set of features in testing stage. The ML is a flashy technology, which is majorly categorized by source of the features. Some networks admit features from external data source to the network. Convolution neural network (CNN) type of networks automatically constructs their own features from the given input images. There are several ML are

*Department of Computer Science, Karpagam Academy of Higher Education, Coimbatore, India(ramd.kannan@gmail.com).

†Department of Computer Science, Karpagam Academy of Higher Education, Coimbatore, India (balaji.nv@kahedu.edu.in)

‡KPR College of Arts Science and Research, Coimbatore, India (th.genish@gmail.com)

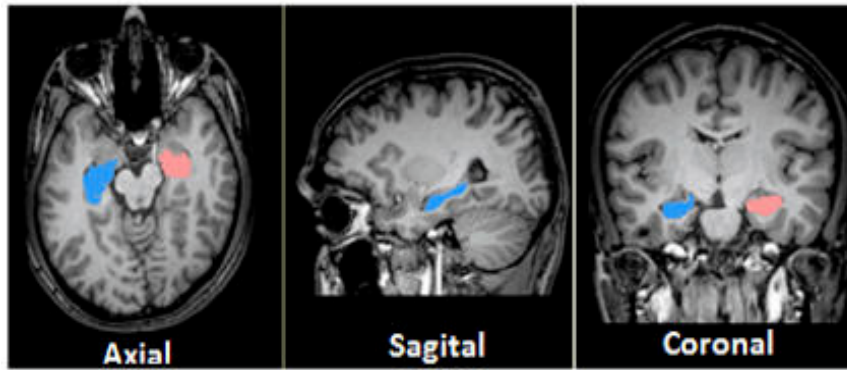


Fig. 1.1: Different MRI image orientation

available such as Support vector machine (SVM), artificial neural network (ANN), CNNetc. and attracted by its accuracy. Several ML methods have been implemented in the task of HC segmentation [3, 4, 12, 24, 25]. Among all, CNN is more compatible for image and employed in HC segmentation from brain MRI [8, 13, 21].

The paper [2] use deep convolution neural network (DCNN) and update the erroneous pixels by error correction steps. Initially, segmentation masks are prepared by using an ensemble models which includes three independent models. The erroneous pixels are corrected by replacing and refining the networks. The method uses several datasets are combined by transfer learning techniques. Thus reduces the time consumption of segmentation process and improves the accuracy of segmentation [2]. In a method, Deep artificial neural network was employed to separate the input image into large patches. The distances between the patches and its regional centroids in compressed images are depicted as feature set [17]. In another CNN model, four gray level patches of a voxel are provided as input to the CNN [10].

The model called Hippodeep proposed by [20] uses CNN and trained in a region of interest (ROI). This model makes use of a single CNN layer, starting with a planar analysis followed by layers of 3D convolutions and shortcut connections. The paper [6] proposed a open source software for the same task. It includes the features obtained from the all orientation MRI images such as coronal, axial and sagittal as given in Fig. 1.1. The combined features fed into U-Net FCNN architecture [17] the network updated with RooNet in [9] to combine two-convolution block of same patch image. The results were finalized after the post processing and obtained 90% dice score [6]. A deep learning method with feed forward learning was used in the segmentation of hippocampus subfield. In the method, a canonical geometrical intensity space is used to reduce the time of pre-processing.

The above stated methods yield good results when using good quality of training images and its truth values. The irregular shape and in-significant boundary of HC provide lower accuracy in results [14]. The presented method selects the very relevant limited features to reduce the memory space and employes multilayer perceptron with back propagation learning algorithm. The following sections describe data set, the validation metrics to analyze the significance of segmentation, methodology, results and discussion and conclusion.

2. Data Set and Valuation Metrics. The experiments carried over Harp and clinical datasets which contains randomly selected 50 patients' images. The axial oriented images only consider for the experiment. The efficiency of a segmentation process is confirmed by computing the Dice Similarity Coefficient (DSC) which is used to compare two segmentation methods (Dice 1945). It can reveal the overlap coefficient between the two different segmented volumes S and G , and is defined in [1] as follows:

$$DSC = 2 \cdot \frac{|S \cap G|}{|S| + |G|} \quad (2.1)$$

S is the region segmented by the automated method and G is the region obtained by manual segmentation. The ' \cap ' operator provides the amount of pixels common to S and G . The '+' operator, produces the sum of all pixels

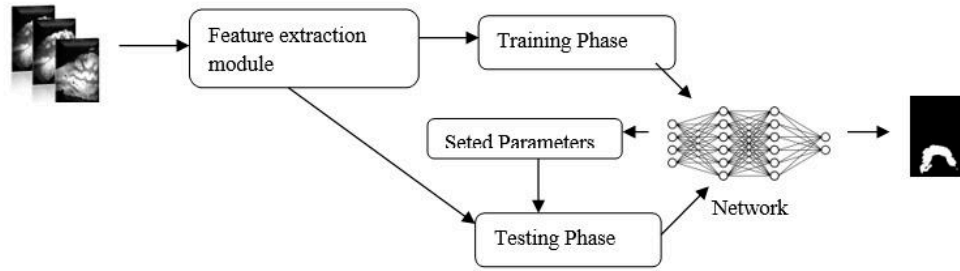


Fig. 3.1: Architectural diagram of presented method

in both regions. The ending value of the DSC is a normalized computation, acquired by the coefficient between the amount of pixels common to both regions and the mean of pixels in each region. The '0' DSC represents no one similar pixel exist in S and G . Controversy, '1' represents the both S and G contain similar pixels.

Sensitivity and specificity are calculated using True positive (TP), False positive (TN) and False negative (FN). Let the pixels inside HCare taken in S and G are positive and background are negative, the TP, TN and FN described as TP = Number of positive pixels in S are in G . FP = Number of positive pixels in S are as negative in G . FN = Number of negative pixels in S are positive in G . The expressions to compute sensitivity and specificity are as follows,

$$Sensitivity = \frac{TP}{TP + FN} \quad (2.2)$$

$$Specificity = \frac{TN}{TN + FP} \quad (2.3)$$

3. Proposed Method. Figure 3.1 shows the architectural diagram of the proposed method. In this module, the input and ground truth images are fed into the feature extraction block at training stage. Twenty types of features recognize and pass as a matrix to the next module. There is a multi-layer perceptron, which is able to understand the feature and train itself to detect the hippocampus pixel by using the feature set. Further, unknown (not included in training image set) image features are given to check its performance. Finally, the net gives output as binary values and are used to construct the output image. The algorithm of the proposed method are given below.

Algorithm

1. start
2. $f = \text{featureExtraction}(\text{image})$ // implement the all formulas given in feature extraction section. //The pixel indexes are taken in row and the features are taken in column
3. $t = \text{truth}(\text{image})$ // assign binary value from the ground truth image
4. // network definition
5. $\text{weights} = [\text{random}()]$
6. // assign net
7. $\text{net} = (\text{layers} = 10, \text{nodes per layer} = 24, \text{activation function} = \text{"sigmoid"})$
8. $x = \text{train}(\text{net}, f, t)$
9. check error values
10. if $\text{error} > \text{previous output}$
11. adjust the weight

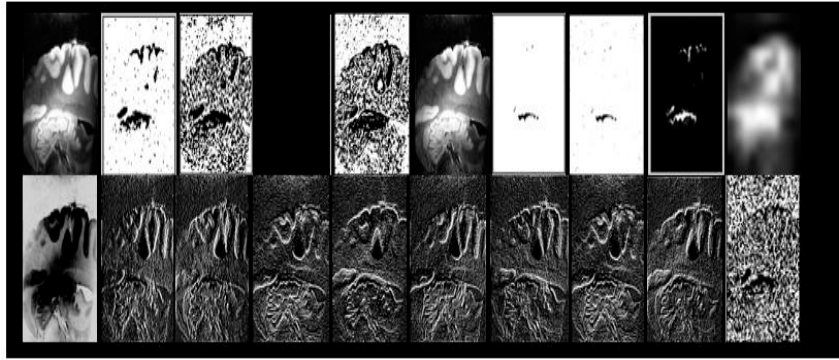


Fig. 3.2: Features of an input image. Row 1: Original image intensity, Skewness using mode, Kurtosis, Mean absolute percentage error, Pixel redundancy, Mean of 5×5 pixel neighbourhood, Variance of 5×5 pixel neighbourhood, Standard deviation of 5×5 pixel neighbourhood, Mean difference and Wavelet feature respectively. Row 2: Energy level, Edge detection filtered images (North, South, East, West, North East, North West, South East, South West) and Standard variation respectively.

12. if (error > previous error)
13. //repeat weight adjustment
14. else
15. // training completed
16. //testing
17. f1=featureExtraction(image)
18. test(net, f1)
19. output the result
20. stop

3.1. Feature Extraction. Features are the numerical or logical representation of image. Each image pixel's association with its neighbourhoods, intensity value and convolution with a filter values are extracted as numerical values and assigned instead of image alone. This method concentrates twenty types of features. The image feature extraction techniques are discussed in the following sections their resulting features are pictorially described in Fig. 3.2.

Skewness: The measure of skewness verifies the symmetry in intensity distribution. The skewness is calculated as follows,

$$f_2 = \frac{\sum_{i,j=1, b=1}^{m,n,k} (I_{i,j} - \bar{I}_b)^3 / N}{S^3} \quad (3.1)$$

Here is skewness obtained from 5×5 neighbourhood of each pixel b . The centre pixel value is replaced with the skewness measure f_1 . $I_{i,j}$ refers the image pixel intensity value, \bar{I}_b represents the mean value of 5×5 neighbourhood of each pixel, N is the total number of pixels here it is takes as 25 and S hold the standard deviation of 5×5 neighbourhood of each pixel. Instead of \bar{I}_b mode and median substituted to obtain skewness mode and skewness median features.

Kurtosis: Kurtosis describes the peakness of a frequency distribution and it is defined as follows,

$$f_3 = \frac{\sum_{i,j=1, b=1}^{m,n,k} (I_{i,j} - \bar{I}_b)^4 / N}{\left(\sum_{i,j=1, b=1}^{m,n,k} (I_{i,j} - \bar{I}_b)^2 / N \right)^2} \quad (3.2)$$

The zero kurtosis represents the normal distribution; the high value distribution reflects the abnormal distribution of intensity value.

Mean Absolute Percentage Error (MAPE): Usually, MAPE utilizes to measure the forecasting error. In image processing, in-homogeneity among a block of pixels derived using MAPE. The error measure by [11]

$$f_4 = \frac{1}{N} \sum_{i=j=1, b=1}^{m, n, k} \frac{(\bar{I}_b - I_{i,j})}{I_b} \times 100 \quad (3.3)$$

The zero result ensures the homogeneity in pixel intensity distribution and high value represent the in-homogeneity proportions with the mean of the block \bar{I}_b .

Pixel Redundancy: The redundant pixels represent the similar object in images. Sometimes pixel redundancy is utilized to denoise image. Here, redundant intensity value of a 5×5 neighbourhood replaces the centre pixel of the block.

$$f_5 = |b_i| \quad (3.4)$$

Mean: The mean of 5×5 neighbourhood pixel replaces the centre pixel value. The calculations performed over the each row and column.

Variance: The variance among 5×5 neighbourhood pixel replaces the centre pixel value. The calculations performed over the each row and column.

Standard deviation: The square root of the variance is called the standard deviation.

Wavelet Feature: The feature is extracted by using discrete wavelet transformation. A brain MRI image is decomposed into n levels until get image size as (15×10) . At this stage, we get a low pass and three high pass filtered images. The low pass filtered image displays distinct intensity at each pixel [11]. At this stage, interpolate the image into its original size of the image. We can see big pixels as given in Fig. 3.1, row 2. The hippocampus and cerebral final fluid (CSF) appearing area looks in high intensity, the others are looks in low intensity as given in [11].

Energy level: The entire work based on the intensity and neighbourhood pixels. The intensity distribution in adjacent regions is categorized as level set. The following mathematical framework helps to extract the energy level of each pixel as defined in [11],

$$f_{12} = \delta(\varphi) \left[\mu \operatorname{div} \left(\frac{\nabla \varphi_{x,y}}{|\nabla \varphi_{x,y}|} \right) - (R(x,y) - C_1)^2 + (R(x,y) - C_2)^2 \right] \quad (3.5)$$

where, f represents the image, $\delta(\cdot)$ is representing Heaviside function, C_1 and C_2 represent the average intensity of pixels above 150 (intensity >150) and below 150 (intensity <150) respectively. The energy level is approximated by the by the Euler Lagrange's formulation. It is defined as,

$$\operatorname{div} \left(\frac{\nabla \varphi}{|\nabla \varphi|} \right) = \frac{\varphi_{xx}\varphi_y^2 - 2\varphi_{xy}\varphi_x\varphi_y + \varphi_{yy}\varphi_x^2}{(\varphi_x + \varphi_y)^{3/2}} \quad (3.6)$$

Edge filters: The edge filters showed in Fig. 3.3 convoluted with the image to obtain edges in all directions individually.

3.1.1. Artificial Neural Network. The presented method uses Multilayer Perceptron with back propagation learning algorithm. It has constructed with more number of layers such as input, hidden and output layers and each layer is holding numerous nodes as described in Fig. 3.4. Each node (neuron) in input layer represents a single feature and includes the connection with n-number of nodes in hidden layer. The nodes act as decision makers with the help of activation functions such as sigmoid, tanh, ReLu and etc. Each neuron calculates the weighted sum of its inputs and then applies an activation function to normalize the sum.

Training: Requirement number of layers, neurons and suitable activation function are determining at the stage of training. Input features and the expected outputs are provided to the network. The network

$$\begin{bmatrix} \begin{bmatrix} -3 & -3 & 5 \\ -3 & 0 & 5 \\ -3 & -3 & 5 \end{bmatrix} & \begin{bmatrix} 5 & -3 & -3 \\ 5 & & -3 \\ 5 & -3 & -3 \end{bmatrix} & \begin{bmatrix} 5 & 5 & 5 \\ -3 & 0 & -3 \\ -3 & -3 & -3 \end{bmatrix} & \begin{bmatrix} -3 & -3 & -3 \\ -3 & 0 & -3 \\ 5 & 5 & 5 \end{bmatrix} & \begin{bmatrix} -3 & -3 & -3 \\ 5 & 0 & -3 \\ 5 & 5 & -3 \end{bmatrix} & \begin{bmatrix} -3 & -3 & -3 \\ -3 & 0 & 5 \\ -3 & 5 & 5 \end{bmatrix} & \begin{bmatrix} 5 & 5 & -3 \\ 5 & 0 & -3 \\ -3 & -3 & -3 \end{bmatrix} & \begin{bmatrix} -3 & 5 & 5 \\ -3 & 0 & 5 \\ -3 & -3 & -3 \end{bmatrix} \end{bmatrix}$$

Fig. 3.3: Edge detection filters, North, South, West, East, South East, North East, South East and North West respectively

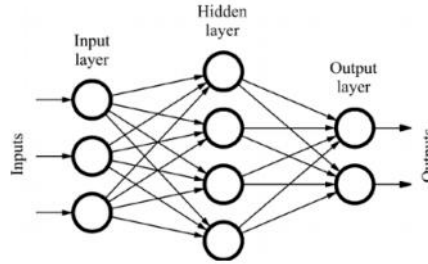


Fig. 3.4: Out sketch of Neural Network

then processes the inputs and compares its outputs against the desired outputs, if fails to give similar output adjust the weights of the network connection until finds the exact results. At the final stage, sets all weights as constant and ready to validate and to run unknown data set.

Testing: At this stage, accepts the unknown image features (not in training set) and set “1” for hippocampus pixels and “0” for non-hippocampus pixels without human intervention.

4. Results and Discussions. The experiment carried over axial brain MRI images data set, which includes three training volumes 1-validation volumes and two testing volumes. The experiment utilizes Harp and clinical dataset and tries to resolve the queries i) finalize the essential features , ii) confirm the fitness of the net iii) Make sure the training package is such that a training image taken from one MRI machine can completely segment the hippocampus from another type of MRI machine.

The experiment commenced with the features skewness, kurtosis, MAPE, pixel redundancy, mean, variance, standard deviation, wavelet features and original intensity. The intensity of hippocampus shows as the Cerebro spinal fluid (CSF) in T2-weighted images. Since the CSF fills in the gap of brain tissues appears as edges, the presented net observes the edges as HC region shown in Fig. 4.1. After the result, we concluded that to include edge features in the training set. For that, the input images convoluted with the eight types of filters individually. When the edge based features included in the training set, the net trained itself and avoid the classification of edge as hippocampus.

Next ensure whether the net is over-fitting or under-fitting, we fitted the net by knowing the accuracy of the training set. Initially, five consecutive images took from each volume and provided at the moment of training which results 0.725 accuracy in 3 epochs.

The architecture of the net determination is the primary problem; minimal number of neuron takes minimal computation time. Initially, one hidden layer consisting of 50 neurons employed for the segmentation which accounts 76% of accuracy. Further, increased the hidden layers as 3 with the same count of neurons as 50. Though, the net is not capacious enough for some complex images. Finally, the neurons are increased for first, second and third layers as 800, 200 and 50 respectively the results are given in Table 4.1. The Table 4.1 shows the highest precision value for the updation of neurons. The Table demonstrated that the net provides lower precision value for 50 neurons and higher precision value for the neuron updated net. Subsequently, the epochs was increased from 5 to 25. At this stage we get lower mean square error value (MSE) 0.0435 and high accuracy

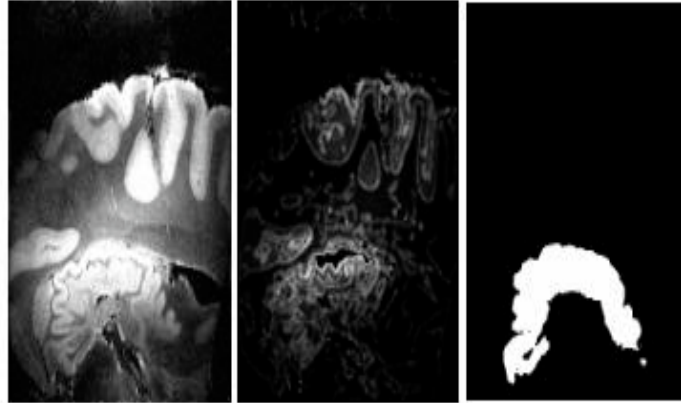


Fig. 4.1: Original image, segmented and ground truth image respectively

Table 4.1: Precision versus Neurons

Training Image	Hidden Layers	Neurons	Highest Precision
10	1	50	76%
15	1	50	70%
20	1	50	62%
10	3	800,200,50	83%
15	3	800,200,50	89%
20	3	800,200,50	94%

as 94%.

The results of modified network by increasing and deleting neurons, layers and epochs have high improvement that is delineated in Fig. 4.2. In Fig. 4.2, the block colour line indicates the performance (DSC score) of the modified net and the gray line indicates (DSC score) of the default net. Y-axis shows the DSC score and X-axis shows the image number.

The sensitivity and specificity of the images illustrated in the Fig. 4.3. In Fig. 4.3, dark line shows the sensitivity and light line shows the specificity. The sensitivity remains the performance of extracting true positive and specificity remains the localization of the work. The obtained average DSC, sensitivity, specificity and standard deviation of the scores are listed in Table 4.2. The sensitivity ranges from 82% to 99% which indicates the proposed features and net can resolve the complex images also. The specificity ranges from 96% to 99% which indicates the net and features incorporate to detect the exact location of hippocampus. The deviations in the results are measured using standard deviation and listed in Table 4.2. In DSC, there are no much deviations among the images of a volume.

The Random forest utilizes the local energy pattern feature set which were proposed in [23] for the classification. The random forest method adopts 20 trees for construction and the depth of each tree is empirically set as 25. The QuickNat network utilizes the convolution neural network for the segmentation process [18] which results lower than the proposed method. The deep learning based method also provided 0.85 DSC score.

Compared to the other method, the proposed feature set and network work similarly and utilizes small data set and less number of feature set. The proposed method takes time for training is 20 minutes and 10 minutes for testing in Dual core 2 machine.

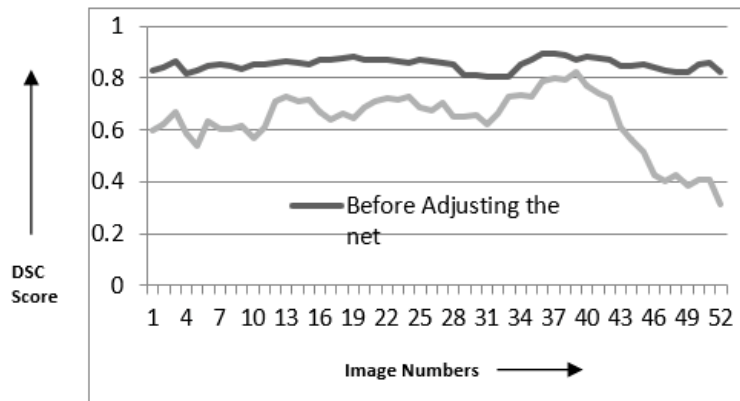


Fig. 4.2: Dice scores of default and modified net

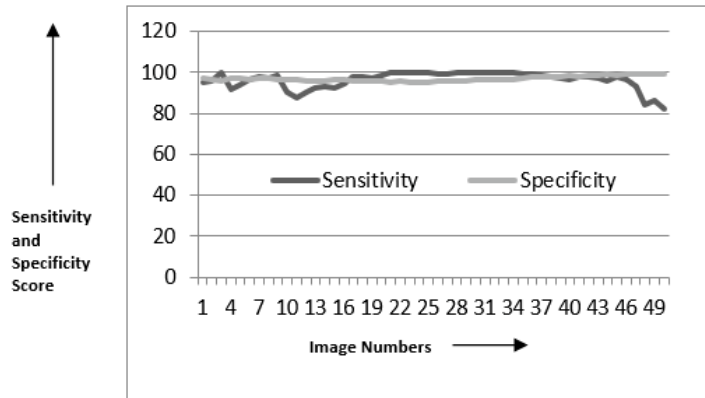


Fig. 4.3: Sensitivity and Specificity of modified net

Table 4.2: Validation measures

	DSC Score	Sensitivity	Specificity
Average	0.851923	96.18962	96.89855
Standard deviation	0.203303	4.288032	1.236299

Table 4.3: Comparison with similar methods

Method	DSC Score
Hippodeep -[20]	0.85
QuickNat -[18]	0.84
Random forest - [3]	0.85
Proposed Method	0.85

The proposed feature set is enough for more images but in two or three images which has connected pixels between CSF and HC lead over-segmentation due to the energy feature.

5. Conclusion. In this paper, we present a multi-layer perceptron framework for hippocampus segmentation from harp and clinical data sets. The network utilizes back propagation learning algorithm. There are twenty features extracted and utilized to set the net. Major advantages of our method lie on that we don't need any time-consuming non-linear registration for pre-processing MR images, and features generated by MDL are consistent with subsequent learning models. The experimental results suggested that the proposed strategically features can boost the performances of hippocampus segmentation and minimize the MSE score. The network model adjusted only based on the MSE error measure and the results are analysed with qualitative and quantitative measures. Sensitivity, specificity, Dice similarity and Accuracy were computed to ensure the outstanding performance of the proposed model. The net model initializes randomly defined weight value for each neuron that increased the training time. In future, initial weight value could be optimized to reduce the overall execution time. As well as more clinical images to be incorporated to achieve the proposed model as reliable one for all configured MRI machine image.

REFERENCES

- [1] KARIM ADERGHAL, KARIM AFDEL, JENNY BENOIS-PINEAU, Gwénaëlle Catheline. Improving Alzheimer's stage categorization with Convolutional Neural Network using transfer learning and different magnetic resonance imaging modalities, *Heliyon*, 6 (2020) e05652
- [2] DIMITRIOS ATALOGLOU, ANASTASIOS DIMOU, DIMITRIOS ZARPALAS, PETROS DARAS, Fast and Precise Hippocampus Segmentation Through Deep Convolutional Neural Network Ensembles and Transfer Learning, *Neuroinformatics* (2019) 17:563–582.
- [3] CAO, L., LI, L., ZHENG, J., FAN, X., YIN, F., SHEN, H., ZHANG, J., 2018. Multi-task Neural Networks for Joint hippocampus Segmentation and Clinical Score Regression. *Multimedia Tools & Applications*, 1st77. Springer, pp. 1–18.
- [4] CAO, P., LIU, X., YANG, J., ZHAO, D., HUANG, M., ZHANG, J., ZAIANE, O., 2017. Nonlinearity-aware based dimensionality reduction and over-sampling for AD/MCI classification from MRI measures. *Comput. Biol. Med.* 91.
- [5] DECARIO L. T. (1997) on the meaning and use of Kurtosis, *Psychological methods*, 2,3, pg. 292-307
- [6] DIEDRE CARMO, BRUNA SILVA. Alzheimer's disease neuro-imaging initiative, Clariss Yasuda, Leticia Rittner, Roberto Lotufo, Hippocampus segmentation on edpilepsy and alzheimer's disease studies with multiple convolutional neural networks, *Heiliyon* 7, 2021, e06226.
- [7] DU A., SCHUFF N., AMEND D., LAAKSO M., HSU Y., JAGUST W., YAFFER K., KRAMER J., REED B., NORMAN D. ET AL. Magnetic resonance imaging of the entorhinal cortex and hippocampus in mild cognitive impairment and alzheimer's disease. *Journal of Neurology, Neurosurgery and Psychiatry*, 71(4), 2001, 441-47.
- [8] CHEN, J., YANG, L., ZHANG, Y., ALBER, M., CHEN, D.Z., 2016. Combining fully convolutional and recurrent neural networks for 3D biomedical image segmentation. *Adv. Neural Inf. Process. Syst.* 3036–3044.
- [9] K. HE, X. ZHANG, S. REN, J. SUN, Deep residual learning for image recognition, in: *Proceedings of the IEEE Conference on Computer Vision and Pattern Recognition*, 2016, pp.770–778.
- [10] F. ISENSEE, P. KICKINGEREDER, W. WICK, M. BENDSZUS, K.H. MAIER-HEIN, Brain tumor segmentation and radiomics survival prediction: contribution to the BraTS2017 challenge, in: *International MICCAI Brainlesion Workshop*, Springer, 2017, pp.287–297.
- [11] S. KARTHIGAI SELVI, 2019. DWT based method to locate tumor from T2-w axial head scan, *international journal of engineering research and applications*, 9,3, pg.63-70.
- [12] LIU, M., ZHANG, J., NIE, D., YAP, P.T., SHEN, D., 2018a. Anatomical landmark based deep feature representation for MR images in brain disease diagnosis. *IEEE J. Biomed. Health Inform.* 22 (3.2), 1476–1485.
- [13] LIU, M., CHENG, D., WANG, K., WANG, Y., 2018B. Multi-Modality Cascaded Convolutional Neural Networks for Alzheimer's Disease Diagnosis, 16. *Neuroinformatics*, pp. 295–308.
- [14] MANHUA LIU, FAN LI, HAO YAN, KUNDONG WANG, YIXIN MA. A multimodel deep convolutional neural network for automatic hippocampus segmentation and classification in alzheimer's disease, *Neuroimage*, 208, 2020, 116459
- [15] ANDREW O'SHEA, RONALD A. COHEN, ERIC C. PORGES, NICOLE R. NISSIM, AND ADAM J. WOODS, Cognitive Aging and the Hippocampus in Older Adults. *Front Aging Neurosci.* (2016).
- [16] TODD MITTON, KAITH VORKINK, Equilibrium underdiversification and preference for skewness, *The financial studies*, 20,4, July 2007, pg.1255-1288.
- [17] O. RONNEBERGER, P. FISCHER, T. BROX, U-Net: convolutional networks for biomedical image segmentation, in: *International Conference on Medical Image Computing and Computer-Assisted Intervention*, Springer, 2015, pp.234–241.
- [18] A.G. ROY, S. CONJETI, N. NAVAB, C. WACHINGER, A.D.N. INITIATIVE, ET AL., Quick-NAT: a fully convolutional network for quick and accurate segmentation of neuroanatomy, *NeuroImage* 186 (2019) 713–727.
- [19] SCOVILLE W.B., MILNER B. Loss of recent memory after bilateral hippocampal lesions. *The journal of neuropsychiatry and clinical neurosciences*, 12(2.1), 2000, 103-a.

- [20] B. THYREAU, K. SATO, H. FUKUDA, Y. TAKI, Segmentation of the hippocampus by trans-ferring algorithmic knowledge for large cohort processing, *Med. Image Anal.* 43 (2018) 214–228.
- [21] WANG, X., GAO, L., SONG, J., SHEN, H., 2017. Beyond frame-level CNN: saliency-aware 3-D CNN with LSTM for video action recognition. *IEEE Signal Process. Lett.* 24, 510–514.
- [22] ZARPALAS D, GKONTRA P, DARAS P, MAGLAVERAS N (2014) Accurate and fully automatic hippocampus segmentation using subject-specific 3D optimal local maps into a hybrid active contour model. *IEEE J Trans Eng Health Med* 2:1–16.
- [23] ZHANG J, LIANG J, ZHAO H (2013) Local energy pattern for texture classification using self-adaptive quantization thresholds. *IEEE Trans Image Process* 22(2.1):31–42
- [24] ZHANG, J., GAO, Y., GAO, Y., MUNSELL, B., SHEN, D., 2016. Detecting anatomical landmarks for fast Alzheimer’s disease diagnosis. *IEEE Trans. Med. Imaging* 35, 2524–2533.
- [25] ZHANG, J., LIU, M., AN, L., GAO, Y., SHEN, D., 2017. Alzheimer’s disease diagnosis using landmark-based features from longitudinal structural MR images. *IEEE J. Biomed. Health Inform.* 21 (3.3), 1607–1616.

Edited by: Vinoth Kumar

Received: Sep 4, 2022

Accepted: Aug 21, 2022